Pulse Radiolysis. The experimental procedures for these measurements have been reported previously.[9a]

Electrochemical Measurements. Cyclic voltammetry was performed with a PAR Model 173 potentiostat in conjunction with a PAR 175 universal programmer. Cyclic voltammograms were recorded on a Houston Instruments Model 2000 x–y recorder. The working electrode was a glassy carbon electrode of area 0.08 cm^2 which had been sealed in heat-shrinkable Teflon. The electrode was cleaned by successive abrasion with Buehler Micropolish A (0.3 micron) and Buehler Micropolish B (0.05 micron) on a polishing cloth, wiping with a Kimwipe, rinsing with water, and air drying. The counter electrode was a carbon rod. The reference electrode was a SCE, and the observed potentials were converted to the NHE by addition of 0.242 V. All measurements were made at 21 ± 1 °C under a nitrogen atmosphere.

Conductivity Measurements. It was found that allowing 1-PrOH to sit in glass resulted in a gradual increase in conductivity. The 1-PrOH was therefore distilled immediately before mixing with triply distilled H_2O (46/54 (w/w)). A standard conductivity cell employing two platinum disks 1 cm in diameter separated by 3 cm in a cell of ~15 mL volume was used. The cell constant was determined by using aqueous KCl solutions. Temperature was controlled at 30.0 ± 0.02 °C with use of a Fisher Water Bath Model 80. Resistance was measured by using a Marconi Instruments Universal Bridge TF2700. The solvent was bubbled with argon before use, and solutions were mixed in a nitrogen-purged glove bag.

Acknowledgment. This work was supported by the National Science Foundation. Stimulating discussions with Jean-Michel Dumas-Bouchiat are acknowledged.

Registry No. 1a, 11077-24-0; **1b**, 92314-56-2; **1c**, 34778-21-7; **1d**, 92314-57-3; **1e**, 51512-99-3; **1f**, 92314-59-5; **1g**, 52633-42-8; **1h**, 92314-61-9; NADH, 58-68-4; [4-^{2}H]NADH, 10012-96-1; [4,4-$^2H_2$]-NADH, 60764-22-9.

Supplementary Material Available: Tables of the rate constants for the oxidation of NADH by ferrocenium ions **1** at varying $NaClO_4$ concentrations and $E°$ values for **1/2** couples at varying $NaClO_4$ concentrations (2 pages). Ordering information is given on any current masthead page.

Binding of the Antitumor Drug *cis*-$[PtCl_2(NH_3)_2]$ to Crystalline $tRNA^{Phe}$ at 6-Å Resolution

John C. Dewan[1]

Contribution from the MRC Laboratory of Molecular Biology, Hills Road, Cambridge CB2 2QH, England. *Received April 30, 1984*

Abstract: Monoclinic crystals of yeast $tRNA^{Phe}$ soaked in reactive hydrolysis products of *cis*-$[PtCl_2(NH_3)_2]$ and in a low chloride ion buffer show drug binding in the vicinity of residues G3-G4, C25-m_2^2G26, G42-G43-A44-G45, and A64-G65. Drug binding invariably results in crystal deterioration with loss of the diffraction pattern beyond a resolution of ~6 Å so that detailed geometric data concerning the binding of the drug cannot be obtained from the present study. Considered together with previous work performed in this area, however, the most probable interpretation of these results is that the *cis*-$[Pt(NH_3)_2]^{2+}$ moiety forms an intrastrand cross-link at certain GG and AG sites within $tRNA^{Phe}$ thereby causing a local distortion of the macromolecule. Features common to each of these binding sites are that at least one G residue is involved, that the adjacent bases in the native undistorted macromolecule are stacked on top of one another, and that the N7 donor atoms of these bases are ~4 Å apart and are not, themselves, involved in hydrogen-bonding interactions elsewhere in the macromolecule. Binding at one CG site is observed and a base-flip by the C residue is invoked to rationalize the drug binding at this site. A preference for the drug to bind at AG rather than GA sites is noted and an explanation offered.

cis-$[PtCl_2(NH_3)_2]$ (*cis*-DDP) is a potent antitumor drug while *trans*-$[PtCl_2(NH_3)_2]$ is inactive.[2-4] There now exists a strong body of evidence[5-14] to suggest that it is the ability of the *cis*-$[Pt(NH_3)_2]^{2+}$ moiety to cross-link between the N7 atoms of two adjacent G residues on the same strand of DNA, and the inability of the trans complex to behave similarly, that is the reason for the diverse pharmacological properties of these two relatively simple inorganic complexes. Since it is the *cis*-$[Pt(NH_3)_2]^{2+}$ moiety that actually forms the cross-link, binding to bipolymers depends very much upon the extent of hydrolysis of the drug and reaction of *cis*-DDP itself is slow compared with the more reactive aquo species such as *cis*-$[PtCl(NH_3)_2(H_2O)]^+$ and *cis*-$[Pt(OH)(NH_3)_2(H_2O)]^+$.[15] It is believed that DNA is the biological target of the drug rather than RNA or protein.[16]

Evidence that the *cis*-$[Pt(NH_3)_2]^{2+}$ moiety forms an intrastrand cross-link with DNA via the N7 atoms of two adjacent G residues stems from several lines of experimentation. First, a greater buoyant density change was seen for poly(dG)·poly(dC) reacted with *cis*-DDP than was observed for platinated poly(dG·dC) when

(1) Present address: Department of Chemistry, Massachusetts Institute of Technology, Cambridge, MA 02139.
(2) "Cisplatin: Current Status and New Developments"; Prestayko, A. W., Crooke, S. T., Carter, S. K., Eds.; Academic Press: New York, 1980.
(3) "Platinum, Gold, and Other Metal Chemotherapeutic Agents"; Lippard, S. J., Ed.; American Chemical Society: Washington, DC, 1983.
(4) "Platinum Coordination Complexes in Cancer Chemotherapy"; Hacker, M. P., Douple, E. B., Krakoff, I. H., Eds.; Martinus Nijhoff Publishing: Boston, 1984.
(5) Lippard, S. J., ref 4, pp 1J–13.
(6) Stone, P. J.; Kelman, A. D.; Sinex, F. M. *Nature (London)* **1974**, *251*, 736.
(7) Kelman, A. D.; Buchbinder, M. *Biochimie* **1978**, *60*, 901.
(8) Tullius, T. D.; Ushay, H. M.; Merkel, C. M.; Caradonna, J. P.; Lippard, S. J., ref 3, pp 51–74 and references therein.
(9) Caradonna, J. P.; Lippard, S. J., ref 4, pp 14–26 and references therein.
(10) Royer-Pokora, B.; Gordon, L. K.; Haseltine, W. A. *Nucleic Acids Res.* **1981**, *9*, 4595.
(11) Girault, J.-P.; Chottard, G.; Lallemand, J.-Y.; Chottard, J.-C. *Biochemistry* **1982**, *21*, 1352.
(12) Girault, J.-P.; Chottard, J.-C.; Guittet, E. R.; Lallemand, J.-Y.; Huynh-Dinh, T.; Igolen, J. *Biochem. Biophys. Res. Commun.* **1982**, *109*, 1157.
(13) Caradonna, J. P.; Lippard, S. J.; Gait, M. J.; Singh, M. *J. Am. Chem. Soc.* **1982**, *104*, 5793.
(14) Eastman, A. *Biochemistry* **1983**, *22*, 3927.
(15) Lim, M. C.; Martin, R. B. *J. Inorg. Nucl. Chem.* **1976**, *38*, 1911.
(16) Roberts, J. J.; Thomson, A. J. *Prog. Nucleic Acid Res. Mol. Biol.* **1979**, *22*, 71.

0002-7863/84/1506-7239$01.50/0

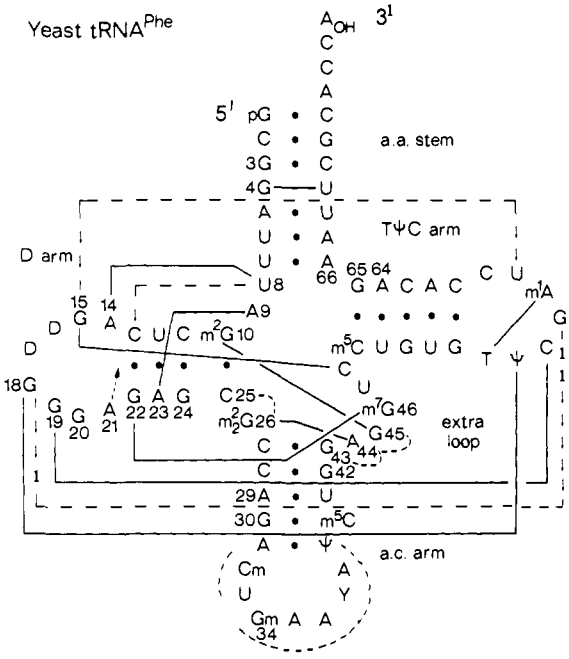

Figure 1. Nucleotide sequence of yeast tRNA^{Phe} arranged in the cloverleaf formula. Solid circles represent Watson–Crick base pairing while other pairs of hydrogen-bonded bases are joined by solid lines. Bases, apart from those in classical Watson–Crick double-helical regions, that stack on one another in the tertiary structure are joined by dashed lines. Hydrogen bonding by A21 to riboses 8 and 48 is indicated by a dashed arrow.

compared to the unplatinated polymers.[6] Second, cleavage of DNA by endonucleases is inhibited by *cis*-DDP binding when the cutting sites have oligo(dG)·oligo(dC) sequences nearby.[7-9] Also, experiments with exonucleases and using DNA sequencing techniques show that DNA cleavage is inhibited at oligo(dG) sites, presumably due to *cis*-DDP binding.[8-10] Third, NMR studies of *cis*-DDP bound to di- and oligodeoxyribonucleotides also provide support for formation of an intrastrand cross-link by *cis*-DDP between adjacent guanine N7 atoms.[11-13] Fourth, recent work on *cis*-DDP binding to DNA followed by chromatographic analysis of the products produced upon DNA degradation strongly suggests that intrastrand cross-linking occurs at GG sites, and also at AG sites.[14]

Thus far direct crystallographic evidence for intrastrand cross-linking in a nucleic acid by *cis*-DDP has not been forthcoming although there now exists quite a large number of small-molecule model compounds having the general formula *cis*-$[Pt(NH_3)_2(purine)_2]^{x+}$ (where purine represents a nucleotide, nucleoside, or nucleobase) that have been structurally characterized.[17-20] Such structures still provide the most accurate geometric data available on the likely *cis*-DDP/DNA adduct although they are by no means ideal models since the purine bases are invariably in a head-to-tail configuration whereas the normal head-to-head configuration would be expected to persist when *cis*-DDP is bound to DNA.[21] The crystal structure of *cis*-DDP bound to an oligonucleotide via the intrastrand cross-linking mode has not yet been obtained. In the model compounds the Pt–N7 distances are always very close to 2.0 Å and the N7–Pt–N7 angle is always close to 90.0°. The dihedral angle between the planes of the purine bases, however, varies from ~40° in nucleotide complexes to ~87° in nucleobase complexes.[18]

Earlier attempts in this laboratory[22] to bind *cis*-DDP to crystalline tRNA^{Phe}, as a model for the drug's binding to DNA, were unsuccessful, and no binding of any kind was observed. *trans*-DDP, on the other hand, gave one strong binding site[22] at the N7 atom of residue Gm34 (Figure 1) and was the best heavy-atom derivative obtained during the solution of the crystal structure of the monoclinic modification of the tRNA. The buffer employed in the experiments with *cis*-DDP had a chloride ion concentration of ~50 mM and the drug was used as the neutral dichloride complex. Under such conditions the concentration of reactive aquo species would be minimal[15] and failure to observe *cis*-DDP binding after a 4-day soak of the crystals at 4 °C is not an unexpected result. The limitations of these earlier crystal soaking experiments were realized in a recent report[23] where orthorhombic tRNA^{Phe} crystals were soaked in a saturated solution of *cis*-DDP for 10 days. Under these more vigorous soaking conditions one drug molecule was found to bind to the N7 atom of residue G15 and a second drug molecule was bound to N7 of G18 (Figure 1). Intrastrand cross-linking was not observed. Crystal-soaking experiments with the self-complementary DNA dodecamer CGCGAATTCGCG and *cis*-DDP resulted in binding at the N7 atoms of three of the inner G residues of the DNA duplex.[24] Binding of *cis*-DDP to the N7 of each G pulls the base out from the helix into the major groove but no intrastrand cross-linking was observed although prolonged soaking eventually led to complete loss of the diffraction pattern. The binding to the three inner G residues was correlated with the ease with which each G residue in the dodecamer can move into the major groove.

This paper presents the results of another study of the *cis*-DDP/tRNA^{Phe} system where the earlier experiments performed in this laboratory[22] have been repeated but with two modifications. The buffer was exchanged for one with a low chloride ion concentration (~8 mM) and the drug was added to the tRNA^{Phe} crystals as a mixture of reactive hydrolysis products[15] (hereafter abbreviated as "activated" *cis*-DDP). It was also reasoned that at least certain GG sequences within tRNA^{Phe} should be accessible to the drug since the $[Co(NH_3)_6]^{3+}$ cation had been shown to bind,[25] via hydrogen-bonding interactions, in the immediate vicinity of residues G3-G4, G42-G43, and A44-G45 (Figure 1). The four binding sites noted in the present work are completely different from the two sites reported in the recent study with the orthorhombic tRNA^{Phe} crystals.[23] Unfortunately, detailed geometric data cannot be obtained from the present work since reaction with the "activated" drug physically degrades the crystals and all diffraction data beyond a resolution of ~6 Å are lost. There is, however, certain useful information that can be gleaned from the study and the work provides the first X-ray structural evidence that *cis*-DDP binds in GG and AG regions of a nucleic acid.

Experimental Section

Crystals of brewer's yeast tRNA^{Phe} were grown by the dialysis method in a manner similar to that described previously.[26] The crystals belong to the monoclinic crystal system, space group $P2_1$, with unit-cell dimensions a = 56.3 Å, b = 33.4 Å, c = 63.0 Å, and β = 90.25°.

The buffer in which the native crystals were stored consisted of 15 mM $MgCl_2$, 10 mM Tris·HCl (pH 7.4), 2 mM spermine·4HCl, and 6% hexane-1,6-diol. Prior to soaking the crystals with "activated" *cis*-DDP this buffer was gradually exchanged for one with a low chloride ion concentration that consisted of 15 mM $Mg(NO_3)_2$, 10 mM KOAc (pH 5.0), 2 mM spermine·4HCl, and 6% hexane-1,6-diol. Crystal quality was not affected by the exchange of buffers.

Hydrolysis products of *cis*-DDP were prepared by overnight stirring of an aqueous suspension of the drug with slightly less than 2 equiv of

(17) Goodgame, D. M. L.; Jeeves, I.; Phillips, F. L.; Skapski, A. C. *Biochim. Biophys. Acta* **1975**, *378*, 153.
(18) Orbell, J. D.; Wilkowski, K.; de Castro, B.; Marzilli, L. G.; Kistenmacher, T. J. *Inorg. Chem.* **1982**, *21*, 813.
(19) Kistenmacher, T. J.; Orbell, J. D.; Marzilli, L. G., ref 3, pp 191–207 and references therein.
(20) Hitchcock, A. P.; Lock, C. J. L.; Pratt, W. M. C.; Lippert, B., ref 3, pp 209–227 and references therein.
(21) den Hartog, J. H. J.; Altona, C.; Chottard, J.-C.; Girault, J.-P.; Lallemand, J.-Y.; de Leeuw, F. A. A. M.; Marcelis, A. T. M.; Reedijk, J. *Nucleic Acids Res.* **1982**, *10*, 4715.
(22) Jack, A.; Ladner, J. E.; Rhodes, D.; Brown, R. S.; Klug, A. *J. Mol. Biol.* **1977**, *111*, 315.
(23) Rubin, J. R.; Sabat, M.; Sundaralingam, M. *Nucleic Acids Res.* **1983**, *11*, 6571.
(24) Wing, R. M.; Pjura, P.; Drew, H. R.; Dickerson, R. E. *EMBO J.* **1984**, *3*, 1201.
(25) Hingerty, B. E.; Brown, R. S.; Klug, A. *Biochim. Biophys. Acta* **1982**, *697*, 78.
(26) Ladner, J. E.; Finch, J. T.; Klug, A.; Clark, B. F. C. *J. Mol. Biol.* **1972**, *72*, 99.

$AgNO_3$ and filtering to remove the precipitated AgCl.[15] The solution thus produced was always used within 24 h.

All crystal soaking experiments were performed at 4 °C. "Activated" *cis*-DDP was added to the buffer containing the $tRNA^{Phe}$ crystals over a period of several hours, to prevent crystal cracking, such that the final drug concentration was ~0.5 mM. This concentration represents a *cis*-DDP/$tRNA^{Phe}$ ratio of ~3:1 and a *cis*-DDP/nucleotide ratio of ~0.04. A *cis*-DDP/$tRNA^{Phe}$ ratio of 3:1 appears to be an optimum value to achieve a balance between strong drug binding and crystal destruction since an increase in this ratio led to complete loss of the diffraction pattern as did prolonged soaking. A variety of soaking experiments were performed, but the results presented are drawn from two experiments one of which represented a 1-week soak and the other a 1-day soak of the $tRNA^{Phe}$ crystals in "activated" *cis*-DDP.

X-ray data to a resolution of 6 Å were collected at −5 °C on a Hilger-Watts four-circle diffractometer. At this limited resolution only one crystal was required per data set. Reaction of the native $tRNA^{Phe}$ crystals with the "activated" *cis*-DDP invariably resulted in the loss of the diffraction pattern beyond 6-Å resolution and also in surface striations on the crystals that run parallel to their long dimension. Native $tRNA^{Phe}$ crystals diffract to 2.5-Å resolution, and a refined structure at this resolution is available.[27] Difference Fourier maps were computed by using coefficients $|F_{Pt}| - |F_{native}|$ and native phases calculated from the 2.5-Å resolution structure.

Results

The 6-Å resolution difference Fourier maps reveal four regions of positive electron density which are the four strongest peaks on the maps and which also represent the only realistic *cis*-DDP binding sites within the $tRNA^{Phe}$ molecule (Figures 1 and 2). Unlike previous metal-binding studies,[22,25,28] the difference maps were somewhat noisy and this is most likely a direct result of the partial crystal destruction upon binding of the "activated" drug. Three of the observed peaks are spherical regions of electron density located near residues G3-G4 (Figure 2a), C25-m_2^2G26 (Figure 2b), and A64-G65 (Figure 2d) while the fourth peak is an elongated region of density located near residues G42-G43-A44-G45 (Figure 2c). The positions of the platinum atoms of the bound *cis*-DDP are presumed to be at the centers of the three spherical regions of electron density and the crystallographic coordinates (in Å) of the platinum atoms at these sites are (34.2, 1.7, 49.6) for the G3-G4 site, (43.0, −0.8, 15.8) for the C25-m_2^2G26 site, and (36.2, 12.0, 45.8) for the A64-G65 site.

Distances between the platinum atoms and atoms of the nearby residues in the native undistorted macromolecule, while of limited value, are still of some interest. At the G3-G4 site the closest distances to the tRNA are Pt–N7(G3) = 2.7 Å and Pt–N7(G4) = 2.4 Å while at the A64-G65 site these distances are Pt–N7(A64) = 2.2 Å and Pt–N7(G65) = 2.4 Å. The third region of spherical density is at residues C25-m_2^2G26 where the relevant distances are Pt–C5(C25) = 1.8 Å and Pt–N7(m_2^2G26) = 2.6 Å. The last region of significant electron density is the elongated region which extends in front of the N7 atoms of residues G42-G43-A44-G45. The distances between the four N7 atoms of these residues, again in the native undisturbed molecule, and the elongated region of electron density also tend to be in the 2–3 Å range.

The limited data set in each case has precluded the refinement of any positional or occupancy parameters. The same contour levels, however, have been used in Figure 2, parts a, b, and d, and the fact that these regions of electron density are all of a similar size suggests that the occupancy at these sites is similar after a 1-week soak in "activated" *cis*-DDP. Even after a 1-week soak the occupancy within the elongated region of electron density at G42-G43-A44-G45 (Figure 2c) is lower than that at the other three sites as might be expected for a situation where disordered binding of the drug presumably occurs. After a 1-day soak the same four binding sites are observed but the occupancy at the A64-G65 site is somewhat lower, and it is interesting that $[Co(NH_3)_6]^{3+}$ does not bind at this site,[25] suggesting that access to the site may be restricted.

Discussion

Taken alone the results of the present work are not easily interpreted in detail. In the light of the previous extensive work[2-14] performed in this area, however, the most likely interpretation is that *cis*-DDP, or more precisely the *cis*-$[Pt(NH_3)_2]^{2+}$ moiety, is cross-linking between adjacent N7 donor atoms of residues G3-G4, G42-G43-A44-G45, and A64-G65. A similar situation probably also occurs at C25-m_2^2G26 although such binding at this site requires a base-flip of ~180° by residue C25 so as to make its N3 available for binding to the drug. This is discussed in more detail below.

The present work does not definitively prove that *cis*-DDP forms an intrastrand cross-link between adjacent N7 atoms within $tRNA^{Phe}$. The partial loss of the diffraction pattern, however, is consistent with some form of distortion of the native macromolecule upon binding of the drug. The exact nature of the binding, and thus of the distortion of the native $tRNA^{Phe}$, cannot be deduced unequivocally since at 6-Å resolution it is impossible to detect the positions to which the native macromolecule will have moved upon *cis*-DDP binding. It is to be stressed, therefore, that Figure 2 depicts the electron density due to the bound *cis*-DDP and superimposed upon this is the native and undistorted $tRNA^{Phe}$ molecule where the atomic coordinates have been taken from the native 2.5-Å resolution structure.[27]

As suggested by model compounds[17-20] a certain amount of local distortion[21] of the native tRNA must occur if *cis*-DDP is to form an intrastrand cross-link although that distortion cannot be overly severe otherwise complete loss of the diffraction pattern might have been observed in the present case. This suggests that the situation depicted in Figure 2 is not grossly different from the actual situation at these binding sites and that a relatively minor reorientation of the two bases bound to the drug has occurred. Since the N7 atoms of the undistorted macromolecule are quite close to the electron density representing the platinum atom of *cis*-DDP, binding to these N7 atoms by the drug would seem to be a reasonable interpretation. In this context it is interesting that recent NMR experiments[29] have shown that below 28 °C all central base pairs of the double-helical decamer TCTCGGTCTC complexed with GAGACCGAGA remain intact, even after *cis*-DDP cross-linking at the GG site, which suggests that distortion of DNA upon drug binding may not be as severe as once thought.

Metal binding to crystalline $tRNA^{Phe}$ does not normally result in crystal deterioration,[22,25,28] and data to 3-Å resolution can be collected in most cases. Studies with $[Co(NH_3)_6]^{3+}$ and *trans*-DDP have been detailed above. Indeed, it is the basis of the multiple isomorphous replacement method,[30] used to solve most protein crystal structures, that metal ions bind with a minimum of disruption to the native macromolecule. Binding by *cis*-DDP in the present case, therefore, represents a situation where a more severe distortion of the macromolecule has occurred but that distortion is not severe enough to destroy completely the crystalline order of the sample and hence to destroy completely the diffraction pattern. This is not consistent with *cis*-DDP binding to the tRNA via hydrogen-bonding interactions alone, or covalently at a single site, but it is quite consistent with the intrastrand cross-linking hypothesis.

If intrastrand cross-linking by *cis*-DDP is occurring at the four binding sites noted in the present work, then certain useful observations concerning the binding of the drug can be made. An examination of the native undistorted $tRNA^{Phe}$ at these binding sites reveals several similarities between them and suggests features within the tRNA, and presumably also DNA, that are required for drug binding. These similarities are that at each of the binding sites at least one G residue is involved and that all the binding sites occur in regions where the bases in the native structure, and on the same strand, are stacked on top of one another and where

(27) Hingerty, B.; Brown, R. S.; Jack, A. *J. Mol. Biol.* **1978**, *124*, 523.
(28) Brown, R. S.; Hingerty, B. E.; Dewan, J. C.; Klug, A. *Nature (London)* **1983**, *303*, 543.
(29) den Hartog, J. H. J.; Altona, C.; van Boom, J. H.; van der Marel, G. A.; Haasnoot, C. A. G.; Reedijk, J. *J. Am. Chem. Soc.* **1984**, *106*, 1528.
(30) Green, D. W.; Ingram, V. M.; Perutz, M. F. *Proc. R. Soc. London, Ser. A* **1954**, *A225*, 287.

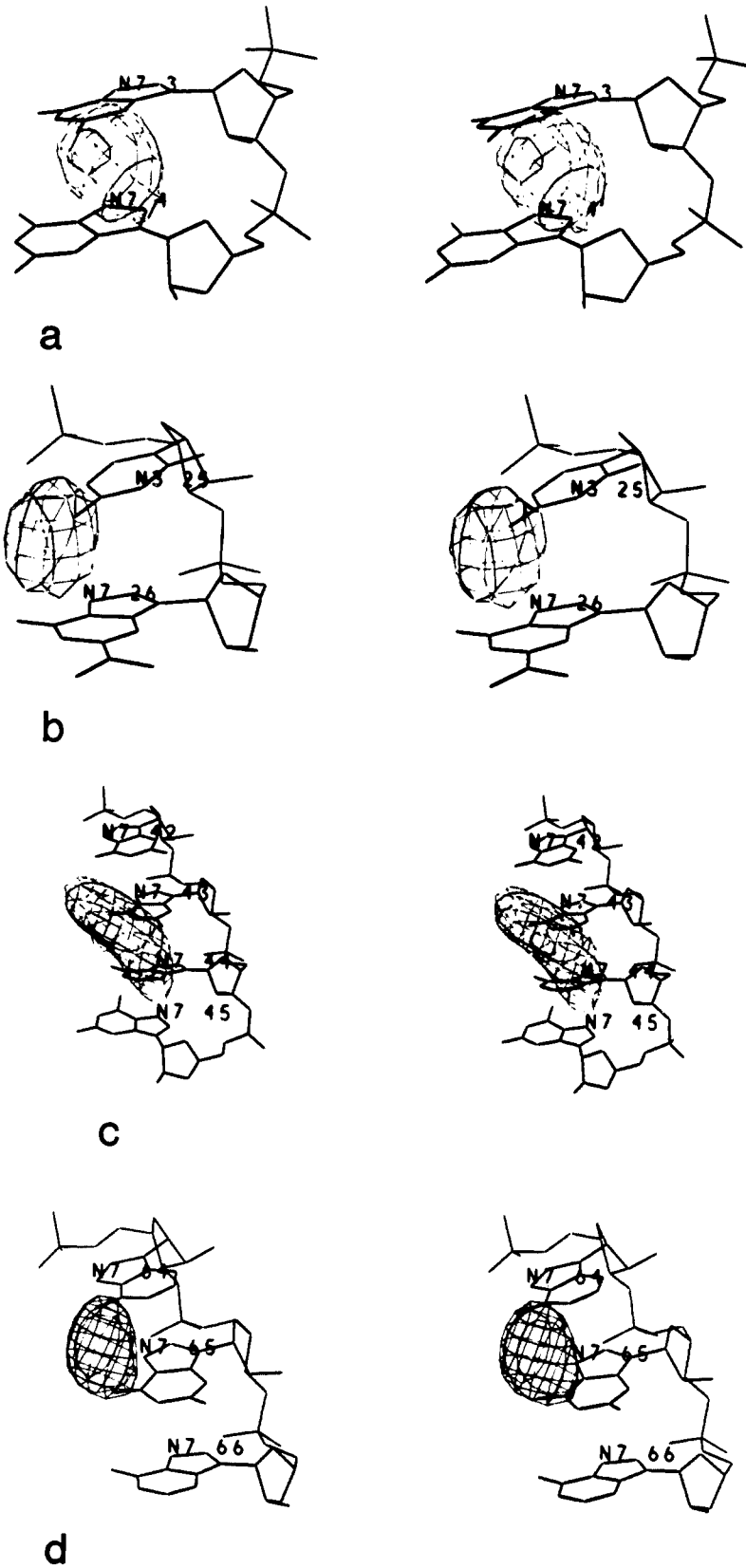

Figure 2. Stereoviews of the four *cis*-$[PtCl_2(NH_3)_2]$ (*cis*-DDP) binding sites in crystalline $tRNA^{Phe}$ after a 1-week soak period. The difference electron density is displayed along with the atom positions of the native undistorted macromolecule taken from a refinement of the native structure at 2.5-Å resolution. Atom labels include the number of the residue to which the labeled atom belongs. (a) The G3-G4 site; (b) the C25-m_2^2G26 site; (c) the G42-G43-A44-G45 site; (d) the A64-G65 site with the AGA sequence A64-G65-A66 being depicted.

the donor atom separation is ~4 Å. The fact that the bases are stacked on one another means that the lone-pair orbitals, on the donor atoms of the residues involved, are each directed in approximately the same sense. These stereochemical conditions at these binding sites do not necessarily imply classical Watson–Crick double-helical regions in the $tRNA^{Phe}$ structure but, in the case of DNA, would most readily be met in such regions.

The stereochemistry of the native $tRNA^{Phe}$ at three of the *cis*-DDP binding sites (Figure 2, parts a, c, and d) suggests that the drug should show a strong preference for binding to AG rather

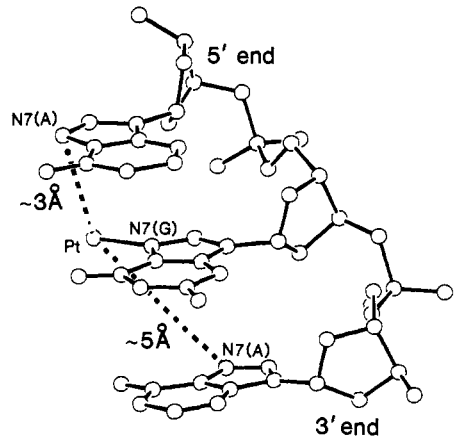

Figure 3. Diagram of an AGA sequence in B-DNA depicting a platinum atom bound to N7 of the G residue where Pt–N7(G) = 2.0 Å. The platinum atom is ~3 Å from N7 of the A residue to its 5′ side and ~5 Å from N7 of the A residue to its 3′ side. Reaction to produce an intrastrand cross-link at the AG site will be strongly favored over that to form an intrastrand cross-link at the GA site.

than GA sequences. The explanation is as follows. It is known that *cis*-DDP will react with G residues faster than with any of the other nucleic acid bases,[31-33] and with A residues next fastest. Therefore, in regions of DNA or RNA possessing the geometry required for drug binding and having, for example, the sequence AGA (Figures 2d and 3), the drug will bind first to the G residue. The platinum atom of the drug is then ~3 Å from the N7 of the A residue to its 5′ side and is ~5 Å from the N7 of the A residue to its 3′ side and reaction at the former site will be strongly favored (Figure 3). That the vast majority of lesions are indeed AG and not GA has been noted in recently published experiments[14] where the ratio of *cis*-DDP binding to AG vs. GA sequences was found to be 90:10. The sequence preference displayed by *cis*-DDP for AG sites also suggests why intrastrand cross-linking was not observed in the crystallographic study of *cis*-DDP binding to the self-complementary DNA dodecamer CGCGAATTCGCG.[24] There is one GA site but no GG or AG sites in that oligonucleotide.

The four binding sites observed in the present work are completely different from the two sites observed in the recent work using orthorhombic crystals of the tRNA.[23] The major differences between these two studies are the low chloride ion concentration and use of reactive hydrolysis products of *cis*-DDP in the present study. It was suggested that the species bound at the N7 atoms of G15 and G18 in the previous work[23] was *cis*-$[Pt(NH_3)_2(H_2O)]^{2+}$, with the fourth site on platinum coordinated to N7 of the G residue. Given the relatively high chloride ion concentration and use of the neutral drug in that work, however, it is more likely that the species bound to the tRNA is *cis*-$[PtCl(NH_3)_2]^+$ and that in the present work the species binding to the tRNA, at least initially, is *cis*-$[Pt(NH_3)_2(H_2O)]^{2+}$. Recent NMR work[34] lends experimental support to this suggestion. One explanation for the completely different binding sites observed in these two studies may lie in the difference in positive charge between the major species expected to be present in solution. In general, species with a higher positive charge should be present in the soaking solutions in the present work,[15] and these may more readily interact with the negatively charged tRNA. It is also worth noting that if the species that initially binds to the tRNA is *cis*-$[Pt(NH_3)_2(H_2O)]^{2+}$, rather than *cis*-$[PtCl(NH_3)_2]^+$, where both the H_2O and Cl^- ligands will be cis to the initial nucleic acid binding site in both of these cases, a second reaction to produce an intrastrand cross-link is far more likely in the former case since a purine N7 atom will displace H_2O from Pt^{2+} about 70 times more rapidly than it will displace Cl^-.[15] The fact that the crystals used in these experiments belong to different crystal systems, and hence exhibit different molecular packing, could be another reason for the different observed binding sites although this would seem to be a less likely explanation. In the present work all four binding sites appear to represent situations where intrastrand cross-linking by *cis*-DDP is occurring and no single site binding is observed. At low drug concentrations this situation has also been noted elsewhere.[14]

As discussed above, the crystallographic results at 6-Å resolution are consistent with intrastrand cross-linking by *cis*-DDP at the G3-G4 and A64-G65 sites. A more complex situation is found at the G42-G43-A44-G45 site where an elongated region of electron density extends in front of the N7 atoms of these four bases (Figure 2c). Two $[Co(NH_3)_6]^{3+}$ cations have also been observed[25] to bind in this region suggesting that the site is quite accessible. There are two ways to interpret the drug binding at this site. First, the elongated region of electron density may be the resultant effect of intrastrand cross-linking at G42-G43 and/or A44-G45 in some of the $tRNA^{Phe}$ molecules in the crystal and at G43-A44 in other of the molecules. Second, the G43-A44 lesion is not favored, according to the sequence preference rules noted above, and binding at GA sites is not observed in any other part of the $tRNA^{Phe}$ structure. The electron density in this region may, therefore, arise from binding at G42-G43 and/or A44-G45 with the local distortion introduced by these two lesions being enough to produce the elongated electron density observed.

The last binding site is at C25-m_2^2G26. The crystallographic evidence for intrastrand cross-linking is more convincing at this site than at any of the other sites since the electron density lies directly between the planes of the two bases (Figure 2b). This probably arises because the two donor atoms at this pyrimidine–purine site lie directly on top of one another and less distortion of the macromolecule is necessary upon drug cross-linking compared to that at the purine–purine sites. The interpretation of the binding at this site, however, is also not straightforward. The Pt–N7(m_2^2G26) distance is 2.6 Å while the distance to residue C25 is 1.8 Å. This 1.8 Å refers, however, to atom C5 of residue C25, and binding to this atom under the present conditions is highly unlikely. It is also unlikely that the binding is to atom N4 of C25. Binding of metal species to such exocyclic amines is not observed in model compounds because the lone pair of electrons on N4 is involved in the π-system of the C ring and is not available for metal coordination.[17] The most plausible explanation for the binding at this site is that the Watson–Crick hydrogen bonds involving C25 have been broken and that the base undergoes a rotation of ~180° about the N1 to C4 axis. This will bring N3 into the position originally occupied by C5, and vice versa. Binding of the drug to N3 of residue C25 is quite acceptable although in double-helical DNA, as in the tRNA, this atom is not normally accessible to metal species. Residue C25 is at the end of a short double-helical section within the D-arm of $tRNA^{Phe}$. "Fraying" at similar sites has been observed[35] in NMR experiments of oligonucleotides down to −30 °C although it has not been observed or suggested before in $tRNA^{Phe}$, especially in the crystalline state. One further point to be considered, however, is that residues C25 and G45 are both hydrogen bonded to m^2G10 and that m_2^2G26 is hydrogen bonded to A44 (Figure 1). *cis*-DDP binding at the G42-G43-A44-G45 site may lead to disruption of the macromolecule in the region around C25-m_2^2G26 which might in turn facilitate or even cause such "fraying". A recent CIDNP study has shown that m_2^2G26 is quite accessible to solvent.[36] The likelihood that C25 was placed up-side-down in the original determination of the native crystal structure is remote.

Apart from the four *cis*-DDP binding sites observed in this work there are several other regions in $tRNA^{Phe}$ where drug binding might be expected at GG or AG sites but is not observed. At

(31) Robins, A. B. *Chem.-Biol. Interact.* **1973**, *6*, 35.
(32) Munchausen, L. L.; Rahn, R. O. *Biochim. Biophys. Acta* **1975**, *414*, 242.
(33) Johnson, N. P.; Hoeschele, J. D.; Rahn, R. O. *Chem.-Biol. Interact.* **1980**, *30*, 151.
(34) Dijt, F. J.; Canters, G. W.; den Hartog, J. H. J.; Marcelis, A. T. M.; Reedijk, J. *J. Am. Chem. Soc.* **1984**, *106*, 3644.
(35) Patel, D. J.; Hilbers, C. W. *Biochemistry* **1975**, *14*, 2651.
(36) McCord, E. F.; Morden, K. M.; Tinoco, I.; Boxer, S. G. *Biochemistry* **1984**, *23*, 1935.

A29-G30 (Figure 1) there is no obvious reason for the lack of drug binding. The explanation that this site is inaccessible seems unlikely since an osmium complex has been observed to bind covalently to the N7 atom of G30.[22] Other workers have observed regions of DNA where drug binding was expected but not observed.[37] In that case incubating the DNA with ethidium bromide prior to reaction with the drug resulted in the expected binding at a 5′-$(dG)_6$-dC-$(dG)_2$-3′ site. At A14-G15 in $tRNA^{Phe}$ the N7 atom of A14 is involved in a reverse Hoogsteen base pair with N3 of U8 which is probably the reason for the lack of drug binding at this site. At A21-G22-A23-G24 the N7 of G22 is hydrogen bonded to N1 of m^7G46 and the N7 of A23 is hydrogen bonded to N6 of A[38,39] which presumably prevents drug binding in this region. *cis*-DDP intrastrand cross-linking at G18-G19-G20 would not be expected since the bases are not stacked on one another and the N7 atoms of adjacent bases are a considerable distance apart [N7(G18)···N7(G19) = 8.1 Å; N7(G19)···N7(G20) = 10.0 Å]. Also residue G57 intercalates between G18 and G19 which will certainly prevent drug cross-linking between these latter two bases. At A9-m^2G10 the donor atom–donor atom distance is rather long to allow intrastrand cross-linking [N7(A9)···N7-(m^2G10) = 6.4 Å]. Drug binding is not observed at A35-A36 or at A66-A67 even though the geometry at these two sites appears to be favorable for binding which suggests that one G residue is required for intrastrand cross-linking, at least at the concentrations used in the present work. Binding is also not observed at A36-Y37 even though Y37 is, in effect, a modified G residue. Certainly the geometry at this site should not preclude drug binding.

Acknowledgment. I am grateful to Dr. A. Klug for advice and encouragement, Dr. D. Rhodes for providing suitable crystals of $tRNA^{Phe}$, and Johnson Matthey PLC for a gift of *cis*-DDP.

(37) Tullius, T. D.; Lippard, S. J. *Proc. Natl. Acad. Sci. U.S.A.* **1982**, *79*, 3489.
(38) Ladner, J. E.; Jack, A.; Robertus, J. D.; Brown, R. S.; Rhodes, D.; Clark, B. F. C.; Klug, A. *Proc. Natl. Acad. Sci. U.S.A.* **1975**, *72*, 4414.
(39) Jack, A.; Ladner, J. E.; Klug, A. *J. Mol. Biol.* **1976**, *108*, 619.

Communications to the Editor

Ester Side-Arm Participation in a Crystalline Lariat Ether–Sodium Bromide Complex

Frank R. Fronczek,[†] Vincent J. Gatto,[‡] Carlo Minganti,[‡] Rose Ann Schultz,[‡] Richard D. Gandour,*[†] and George W. Gokel*[‡]

Departments of Chemistry
Louisiana State University
Baton Rouge, Louisiana 70803-1804
University of Maryland
College Park, Maryland 20742
Received June 15, 1984
Revised Manuscript Received September 17, 1984

An interesting aspect of ionophore chemistry is that naturally occurring cation carriers utilize ester carbonyl donor groups to complex cations.[1] In this respect, valinomycin[2] is typical. It has six amide carbonyls which are involved in hydrogen bonding around the periphery of the three-dimensional structure and six ester carbonyl groups which bind the cation.[3] Crown ethers have been extensively used as ionophore models even though they generally lack ester linkages.[4] In numerous cases, ester residues have been incorporated,[5] but in 15- or 18-membered rings, the carbonyls must be turned outward, geometrically prohibiting interaction with an intraannular cation. If the ester donor is part of a flexible, lariat ether side arm, this restriction should be lifted. The first X-ray crsytal structure of a lariat ether ionophore in which an ester carbonyl group interacts directly with the ring-bound cation is reported here.

This structure should be viewed in the context of other macrocyclic polyether compounds with side-chain interactions with a metal cation.[6] These laboratories[6a] and others[6b] have reported crystal structures of complexes with side arms containing ether and alcohol oxygens. Other laboratories have reported crystal structures of complexes with carboxamide[6c] and carboxylate[6d] side arms.

The structure of the complex that forms between sodium bromide and ethyl (1-aza-4,7,10,13-tetraoxacyclopentadecyl)-ethanoate[7] (**1**) is shown in Figure 1 along with a skeletal drawing of the donor atoms and the metal. Of the six lariat donor atoms, the ester carbonyl oxygen, O18, is closest to the metal ion. As the skeletal drawing reveals, the five donor atoms of the macroring approximate a half-chair conformation, C_2 symmetry with O7 on the axis. Bromide ion also serves as a donor making Na^+ heptacoordinate in this complex.

[†] Louisiana State University.
[‡] University of Maryland.

(1) (a) Dobler, M. "Ionophores and their Structures"; Wiley: New York, 1981. (b) Hilgenfeld, R.; Saenger, W. *Top. Curr. Chem.* **1982**, *101*, 1-82.
(2) Ovchvinnikv, Yu. A.; Ivanov, V. T.; Shkrob, A. M. "Membrane Active Complexones"; Elsevier: Amsterdam, 1974; pp 118-131.
(3) (a) Ventkatachalam, C. M. *Biopolymers* **1968**, *6*, 1425-1436. (b) Pinkerton, M.; Steinrauf, L. K.; Dawkins, P. *Biochem. Biophys. Res. Commun.* **1969**, *35*, 512-518. (c) Neupert-Laves, K.; Dobler, M. *Helv. Chim. Acta* **1975**, *58*, 432-442.
(4) Gokel, G. W.; Korzeniowski, S. H. "Macrocyclic Polyether Synthesis"; Springer-Verlag: Heidelberg, Germany 1982.
(5) Asay, R. E.; Bradshaw, J. S.; Neilsen, S. F.; Thompson, M. D.; Snow, J. W.; Masihdas, D. R. K.; Izatt, R. M.; Christensen, J. J. *J. Heterocycl. Chem.* **1977**, *14*, 85-90.
(6) (a) Fronczek, F. R.; Gatto, V. J.; Schultz, R. A.; Jungk, S. J.; Colucci, W. J.; Gandour, R. D.; Gokel, G. W. *J. Am. Chem. Soc.* **1983**, *105*, 6717-6718. (b) Buoen, S.; Dale, J.; Groth, P.; Krane, J. *J. Chem. Soc., Chem. Commun.* **1982**, 1172-1174. Groth, P. *Acta Chem. Scand., Ser. A* **1983**, *A37*, 71-74, 75-77, 283-291. (c) Behr, J.-P.; Lehn, J.-M.; Dock, A.-C.; Moras, D. *Nature (London)* **1982**, *295*, 526-527. Dock, A.-C.; Moras, D.; Behr, J.-P.; Lehn, J.-M. *Acta Crystallogr. Sect. C.* **1983**, *C39*, 1001-1005. (d) Behr, J.-P.; Lehn, J.-M.; Moras, D.; Thierry, J. C. *J. Am. Chem. Soc.* **1981**, *103*, 701-703. Uechi, T.; Ueda, I.; Tazaki, M.; Takagi, M.; Ueno, K. *Acta Crsytallogr., Sect. B* **1982**, *B38*, 433-436. Gluzinski, P.; Krajewski, J. W.; Urbanczyk-Lipkowska, Z.; Bleidis, J.; Misnyov, A. *Cryst. Struct. Commun.* **1982**, *11*, 1589-1592. Gluzinski, P.; Krajewski, J. W.; Urbanczyk-Lipkowska, Z.; Andreetti; G. D.; Bocelli, G. *Acta Crystallogr., Sect. C* **1984**, *C40*, 778-781. Krajewski, J. W.; Gluzinski, P.; Urbanczyk-Lipkowska, Z.; Dobler, M. *Acta Crystallogr., Sect. C* **1984**, *C40*, 1135-1137. Shoham, G.; Christianson, D. W.; Bartsch, R. A.; Heo, G. S.; Olsher, U.; Lipscomb, W. N. *J. Am. Chem. Soc.* **1984**, *106*, 1280-1285. (e) Kulstad, S.; Malmstem, L. A. *J. Inorg. Nucl. Chem.* **1981**, *43*, 1299-1304. Tazaki, M.; Nita, K.; Takagi, M.; Ueno, K. *Chem. Lett.* **1982**, 571-574. Strzelbicki, J.; Bartsch, R. A. *J. Membr. Sci.* **1982**, *10*, 35-47. Behr, J.-P.; Lehn, J.-M.; Vierling, P. *Helv. Chim. Acta* **1982**, *65*, 1853-1867. Shinkai, S.; Kinda, H.; Sone, T.; Manabe, O. *J. Chem. Soc., Chem. Commun.* **1982**, 125-126. Fyles, T. M.; Whitfied, D. M. *Can. J. Chem.* **1984**, *62*, 507-514. Masayuma, A.; Nakatsuji, Y.; Ikeda, I.; Okahara, M. *Tetrahedron Lett.* **1981**, *22*, 4665-4668. Nakatsuji, Y.; Nakamura, T.; Okahara, M. *Chem. Lett.* **1982**, 1207-1210. Tsukube, H. *J. Chem. Soc., Chem. Commun.* **1984**, 315-316. Amble, J. E.; Dale, J. *Acta Chem. Scand., Ser B* **1979**, *B33*, 698-700. Calverley, M. J. *Acta Chem. Scand., Ser. B* **1982**, *B36*, 241-247.
(7) Compound **1** was prepared by alkylation of 1-aza-4,7,10,13-tetraoxacyclopentadecane[8] with ethyl bromoacetate (CH_3CN/Na_2CO_3) in 53% yield. The nearly colorless oil was treated with an equivalent amount of NaBr and crystallized from cold acetone and gave a white solid: mp 114-115 °C; ^1H NMR ($CDCl_3$) δ 1.3 (t), 2.8 (t), 3.5 (s), 3.6 (s), 3.7 (s), 4.2 (q); IR (KBr) 1740-1735 (C=O), 1205, 1115-1105, 1085-1045 (COC) cm^{-1}. Anal. Calcd for $C_{14}H_{27}NO_6BrNa$: C, 41.19; H, 6.84; N, 3.22; Br, 20.10. Found: C, 41.02; H, 6.84; N, 3.22; Br, 20.10.

0002-7863/84/1506-7244$01.50/0